

Microwave Engineering Research Activity in Israel

■ Reuven Shavit, Albert Sabban, Michael Sigalov, Avihai Lahman, Zeev Iluz, Naftali Chayat, and Solon Spiegel

Microwave engineering research activities in Israel began during the 1960s at Rafael, a government-owned research institute, when a motivated and dedicated team of scientists and engineers worked hard to lay the foundation for microwave engineering in Israel. A few years later, more microwave groups were founded, e.g., within Elta, a subsidiary of the Israel Aircraft Industry, and within Elisra, a Ministry of Defense research laboratory. These centers, along with academic research activity at the Technion, Tel-Aviv University (TAU), Ben-Gurion University (BGU), and the Weizmann Institute, led microwave activity for a decade.

Historical Background

In 1977, Israel's first commercial microwave company, Mikrokim, was established as a cooperation between Rafael and U.S.-based MACOM. One of the major scientific contributions performed at Rafael in the early 1970s was the development of software for microwave analysis and design: this pioneering work was led by the late

Reuven Shavit (rshavit@ee.bgu.ac.il) is with the Department of Electrical and Computer Engineering, Ben-Gurion University of the Negev, Beer Sheva, Israel. Albert Sabban (sabban@braude.ac.il) is with the Department of Electrical Engineering, Ort Braude College, Karmiel, Israel. Michael Sigalov is with Panasonic (Israel), Yokneam, Israel. Avihai Lahman is with Gilat Networks, Petah Tikva, Israel. Zeev Iluz is with Department of Physical Electronics, Tel Aviv University, Israel. Naftali Chayat is with Vayyar Imaging, Iehud, Israel. Solon Spiegel is with Rio Systems, Givat Shmuel, Israel.

Digital Object Identifier 10.1109/MMM.2018.2802281
Date of publication: 6 April 2018



©ISTOCKPHOTO.COM/LISANFISA

H. Rabin and performed several years before the development of the first commercial computer-aided design tool, Touchstone, by Compact Software in the United States. During the 1980s, more companies entered the microwave field, such as Optomic, Eyal, and General Motors (Israel).

During the 1990s, many communications start-ups were established, and quite a few more microwave centers initiated, such as CyOptics, Foxcom, Gilat, Helicomm, MTI, Ravon (minicircuits), Motorola, Tadiran, and Intel. In parallel, university microwave engineering education was extended with the addition of faculty members specializing in electromagnetics, and this topic became a specific electrical engineering specialization track, with a structured curriculum at the undergraduate and graduate levels. Basic microwave engineering education was also introduced at Ariel University and in many engineering colleges founded through the 1990s.

The Joint Chapter of the IEEE Antennas and Propagation Society (APS)/IEEE Microwave Theory and Techniques Society (MTT-S) was estab-

lished in Israel in 1973 by A. Madjar with help from L. Young, who was then on sabbatical at the Technion. Since its creation, the Chapter organizes local technical meetings on antennas and microwave engineering every year. Recognizing the high standard of microwave activity in Israel, the European Microwave Conference Management Committee decided to hold the conference in Israel in 1997. S. Auster, who succeeded A. Madjar as Israel's IEEE APS/MTT-S Chapter chair, extended

the local annual microwave and antenna symposium to an international conference, the IEEE Conference on Microwaves, Communications, Antennas and Electronic Systems (COMCAS), which, since 2008, has brought together scientists and engineers around the world. COMCAS is held in Tel-Aviv every other year.

Pioneering activity in microwave integrated circuits (MICs) started at Rafael during the early 1970s and later migrated to other companies (Elisra, Elta, and Optomic, for example). Gallium arsenide (GaAs) monolithic MIC (MMIC) activity began in Israel during the 1980s and increased substantially with the creation of a GaAs consortium in the 1990s. Today, there are established MMIC design groups as well as a GaAs foundry; the microwave activity, initially focused on military applications, drifted toward many commercial applications that cover systems up to terahertz frequencies.

In the following sections, we describe a few antenna and microwave engineering projects developed in Israel that we believe are of interest to the larger antenna and microwave community. The projects are diverse, related to satellite communication, nano-antenna

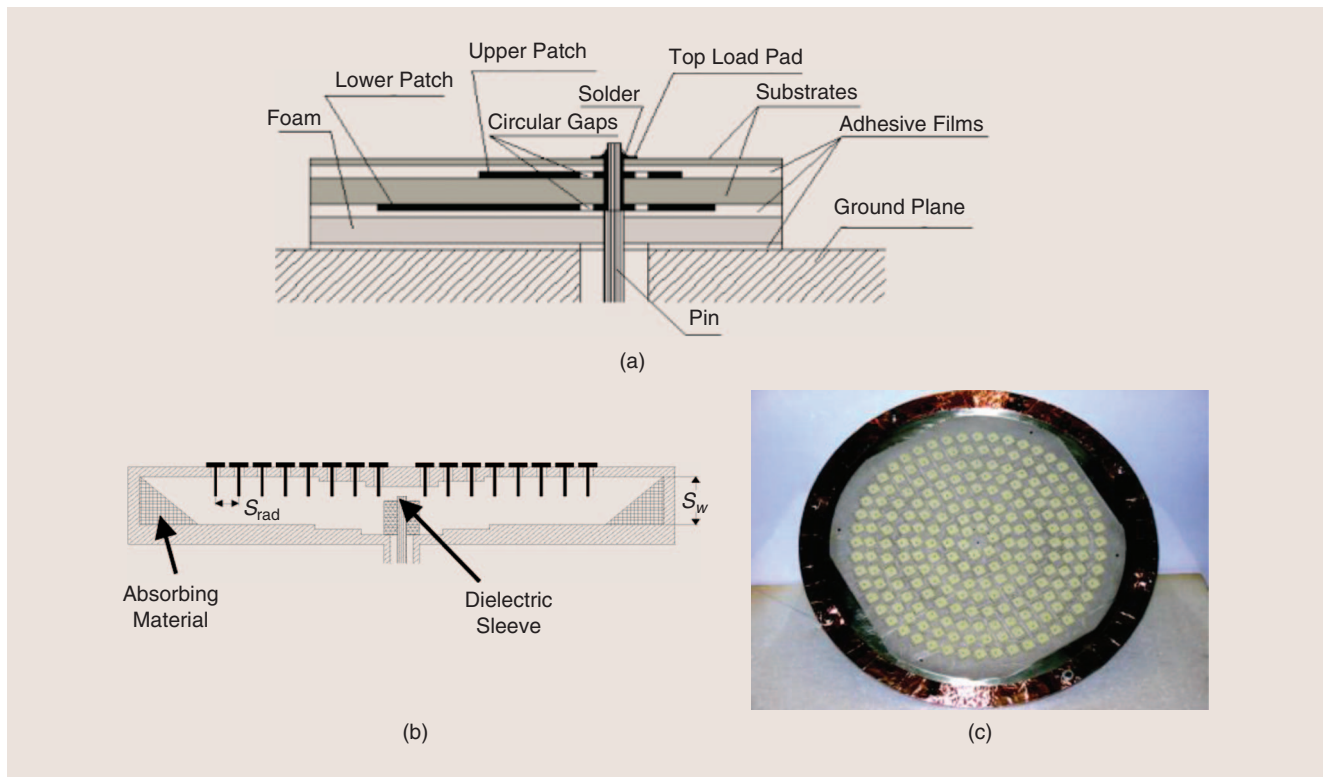


Figure 1. The geometry of the dual-frequency, dual-circular-polarization microstrip antenna: (a) the element, (b) the array cross section, and (c) a photo of the antenna.

technology, wearable antennas for medical applications, and RF integrated circuits (RFICs).

Satellite Communication

We begin by describing three antenna projects related to satellite communications developed at BGU, Technion, Panasonic (Israel), and Gilat.

Dual-Frequency, Dual-Circular-Polarization Microstrip Antenna

The first project was a joint venture between BGU and Technion [1] supported by the Information Super-Highway in Space consortium associated with the Israeli Trade and Industry Ministry. This work involved the development of a fixed-beam, dual-frequency (Ku-band) circular array with dual circular polarization based on printed elements fed by a radial network. The radial line-feeding network was chosen to reduce the antenna losses encountered with a standard microstrip conformal network and is based on two stacked circular patches fed in tandem by a single pin, as shown in Figure 1(a). Circular polarization was achieved for each

circular patch by introducing two indents in the patch. To reduce mutual coupling among the array's elements through surface-waves coupling, the elements were truncated to a square $12\text{ mm} \times 12\text{ mm}$, as shown in Figure 1(b). The elements in the array are arranged in concentric circles and fed through pins embedded in the radial line. The radial line is fed through a probe at its center. A prototype of the array with eight rings and a diameter of 30 cm has been built [Figure 1(c)].

The antenna was tested, and a comparison between the simulated and measured results of the far-field radiation patterns showed nice agreement. The measured gain obtained at 12.3 GHz was 26 dBic and at 14 GHz was 27 dBic. The measured axial ratio in the receive (Rx) band (10.9–12.7 GHz) is lower than 1 dB and in the transmit (Tx) band (14–14.5 GHz) lower than 2 dB. The aperture radiation efficiency was higher than 65% in both frequency bands.

IFEC Antenna Solutions

The second project was developed at the Antenna Development Center (ADC) of

Panasonic Avionics Corporation (PAC) in Israel and manufactured at PAC's Lake Forest facilities in California. PAC is a world leader in in-flight entertainment and connectivity (IFEC) solutions and has the only global, broadband in-flight connectivity service operating over every country around the world today. ADC has developed two satellite communications (SatCom) Ku-band antennas, a dual-panel antenna (DPA), and a single-panel antenna (SPA).

Both antennas provide elevation over azimuth electromechanical steering, with fully electronic polarization tracking, while supporting concurrent, dual-linear polarization or circular polarization in Rx and linear polarization on Tx. The DPA system is installed on more than 1,600 commercial aircraft. The SPA was launched for commercial use in 2015 and has only one antenna array. The SPA structure and its radiation pattern are shown in Figure 2. It is lighter, easier to manufacture, and less expensive and also offers higher reliability than previous IFEC solutions.

The SPA (on ground) measured gain-to-noise temperature (G/T) is 12.5 dB/°K

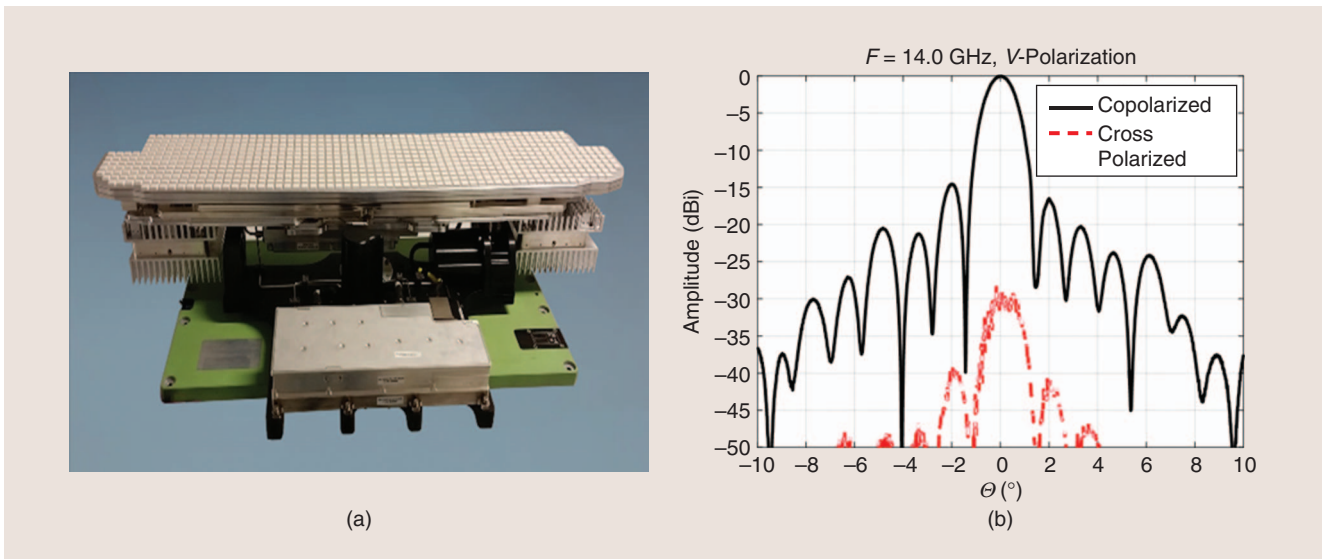


Figure 2. (a) The SPA PAC system and (b) the SPA radiation pattern at 14 GHz.

at 11.7 GHz, and the 3-dB beamwidth of the antenna is 1.3° at 14.0 GHz. The measured gain obtained at 12 GHz was 34 dBi and at 14.25 GHz was 36 dBi. To minimize the RF losses and maximize the system G/T, the SPA is divided into four quarters. Four broadband diplexer modules are connected to the antenna quarters and provide greater than 900-dB isolation between the Tx and Rx signals. The Rx signals from the antenna quarters are amplified with four low-noise amplifiers (LNAs), combined and processed in the polarization setup circuitry. The Tx signal is amplified with two high-efficiency GaN power amplifiers (PAs) and connected to the antenna quarters through two four-way waveguide dividers.

High-Capacity Satellite Ku-/Ka-Band Antenna

The third project, developed by Gilat, is a high-capacity satellite Ku-/Ka-band antenna with advanced network features that have revolutionized in-flight connectivity. This system is an innovative two-way antenna system that can be switched between Ka- and Ku-bands during flight and can operate in either band as required. This solution enables aeronautical real-time broadband satellite communications for video, voice, and data. A photo of the developed antenna is shown in Figure 3.

The antenna maximizes throughput using high-efficiency waveguide panel technology. Its low profile and light weight also ensure easy and safe mounting on aircraft. The antenna has been uniquely designed as an integrated dual-band (Ka and Ku) antenna system. Ideal for seamless transition between regional (Ka) and transatlantic (Ku) coverage, the system allows easy and quick electronic switching between frequency bands, without requiring any disassembly or component replacement. It enables maximum Ka-/Ku-band satellite network data rates and provides a superior antenna system performance in Tx and Rx.

The Ka antenna panel is capable of operating across the entire K-band (17.7–20.2 GHz) and Ka-band (25.7–30.0 GHz) for civil communications. Tapered amplitude distribution contributes to efficient radiation pattern at Tx frequencies. The Ku panel design supports the downlink frequency range of 10.7–12.75 GHz and uplink band of 13.75–14.5 GHz. Flexible control of the polarization allows for offset compensation of the linearly polarized signals as well as the ability to receive and transmit circular polarizations. The measured gain and cross polarization in the Tx band at 14.25 GHz are 33 dBi and -40 dB, respectively, and its G/T in the Rx band at 11.5 GHz is 11 dB/K. The measured gain and cross polarization in

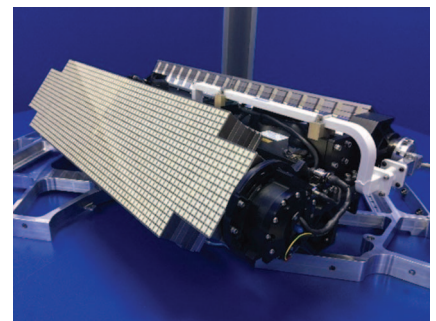


Figure 3. The dual-panel Ku-/Ka-band Gilat SatCom antenna.

the Tx band at 29 GHz are 39.8 dBic and -26 dB, respectively, and its G/T in the Rx band at 19.2 GHz is 13.5 dB/K.

Nano-Antenna Technology

Considerable work has recently been devoted to nano-antennas for the infrared and optical frequencies. Due to its extremely small dimensions and high losses, it is impossible to measure nano-antenna impedance directly by connecting probes or transmission lines to the antenna terminals. For this purpose, a different approach was adopted at TAU for characterizing the nano-antenna, based on external illumination of an antenna array with different loads and measurements of the scattered fields [2]–[4].

One option for an efficient broadband nano-antenna involves the use of two end-fire antennas (Vivaldi),

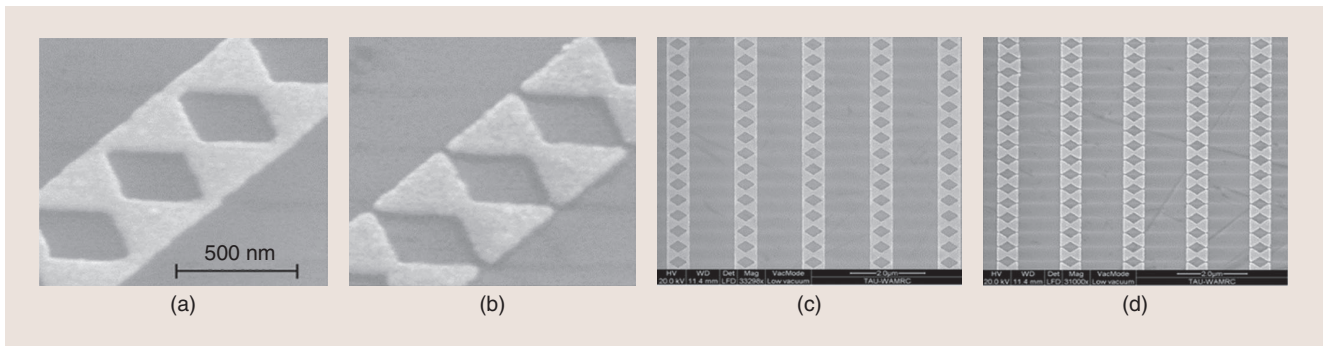


Figure 4. SEM images of the fabricated (a) short-circuit array and (b) open-circuit array. (c) and (d) show zoom outs of the arrays.

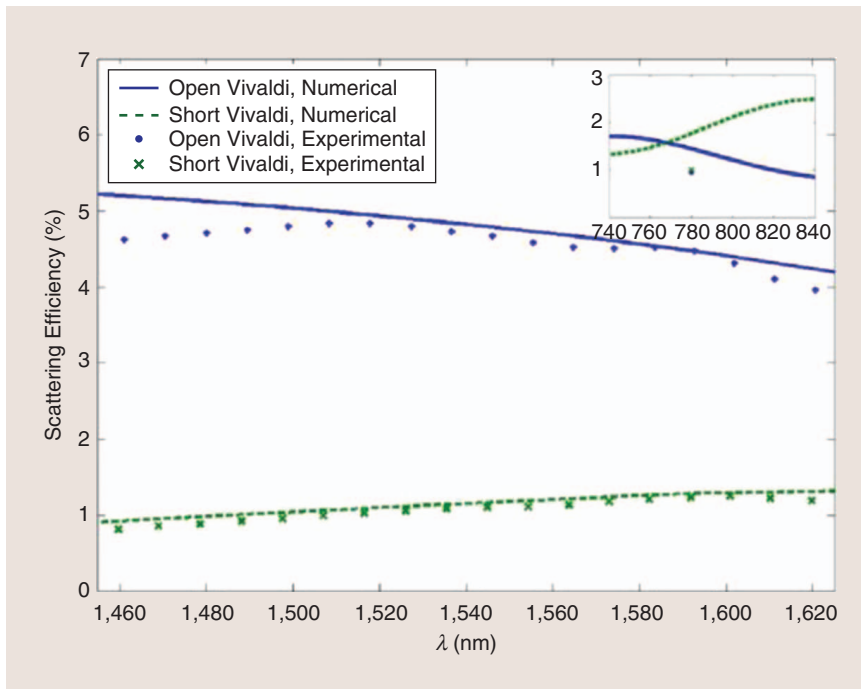


Figure 5. The antenna scattering efficiencies as a function of wavelength.

placed opposite to one another, so as to get a peak gain at the antenna's broadside direction. The antennas were fabricated with electron-beam lithography on quartz. The dual Vivaldi antenna array was fabricated with both open-circuit and short-circuit termination. Scanning electron microscope (SEM) images of the two fabricated arrays are presented in Figure 4. To characterize the antennas, the arrays were illuminated by a collimated beam. The sample was placed on a rotation positioner, which controlled the alignment of the sample relative to the incident light.

The scattering efficiencies of both antenna configurations are presented

in Figure 5, where they are compared to the numerical simulation results (only one of several lobes is shown). The antenna's total radiation efficiency (all lobes) is approximately 94%.

Wearable Antennas for Communication and Medical Systems

Metamaterial and fractal technology is used to improve the efficiency of small antennas, as presented in [5]–[7]. The gain of the patch antenna with split-ring resonators (SRRs) is higher by 2.5 dB than the antenna without SRRs. The resonant frequency of the antennas with the SRR is lower by 5–10% than the antennas without SRR. Fractal antennas are very com-

pact and multiband, and they have useful applications in RF systems.

Wearable Antenna Based on SRR

A dual-polarized antenna with an SRR is shown in Figure 6(a). The microstrip loaded dipole with SRR provides horizontal polarization, and the slot antenna provides vertical polarization. The resonant frequency of the antenna with SRR is 400 MHz; the resonant frequency of the antenna without SRR is 10% higher. The S_{11} and the antenna gain are presented in Figure 6(b). Metallic strips have been added to the antenna with the SRR, as presented in Figure 7(a). The antenna gain and the S_{11} of the antenna with metallic strips are presented in Figure 7(b). The antenna feed network was optimized to yield a voltage standing wave ratio (VSWR) better than 2:1 in the frequency range of 250–420 MHz.

Wearable Antenna Based on Fractals

A new fractal wearable antenna approach is presented in Figures 7(c) and 8(c). The antenna resonator was printed on a substrate 0.8-mm thick with a 2.2 dielectric constant. The patch radiator was printed on an FR4 substrate 0.8-mm thick. The antenna dimensions are 45.8 mm × 39.1 mm. The VSWR of the fractal antenna with 2-mm air spacing between the layers is better than 2:1 for 10% bandwidth. The antenna beamwidth is approximately 82°, with 7.5 dBi gain.

RFIC: System-on-Chip for MIMO Radar

Vayyar Imaging Ltd. has developed the VYYR2401 Octopus multichannel

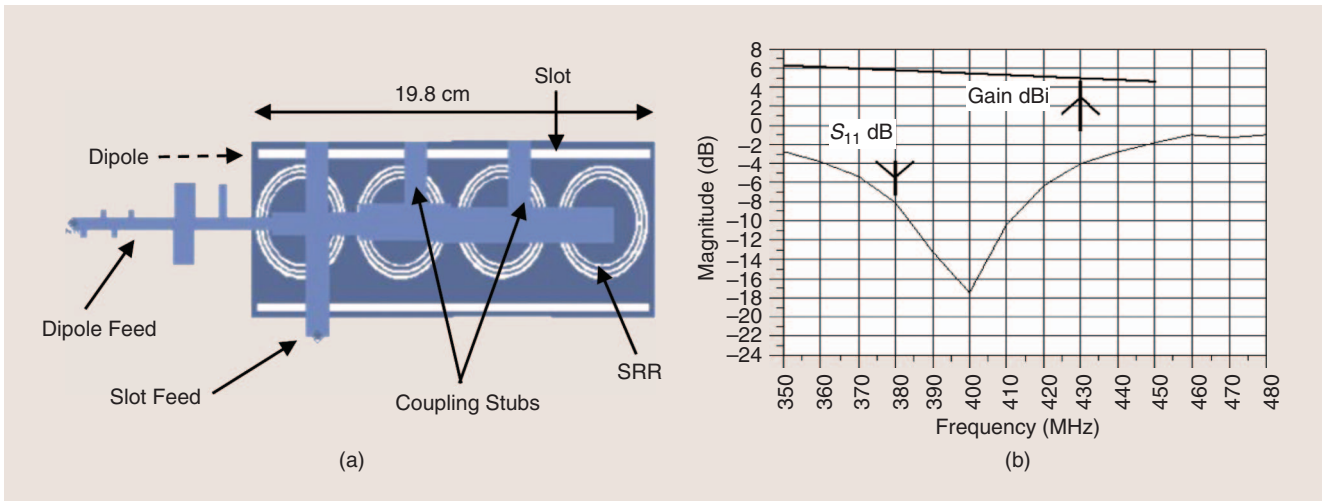


Figure 6. (a) The printed antenna with an SRR and (b) the computed S_{11} and antenna gain.

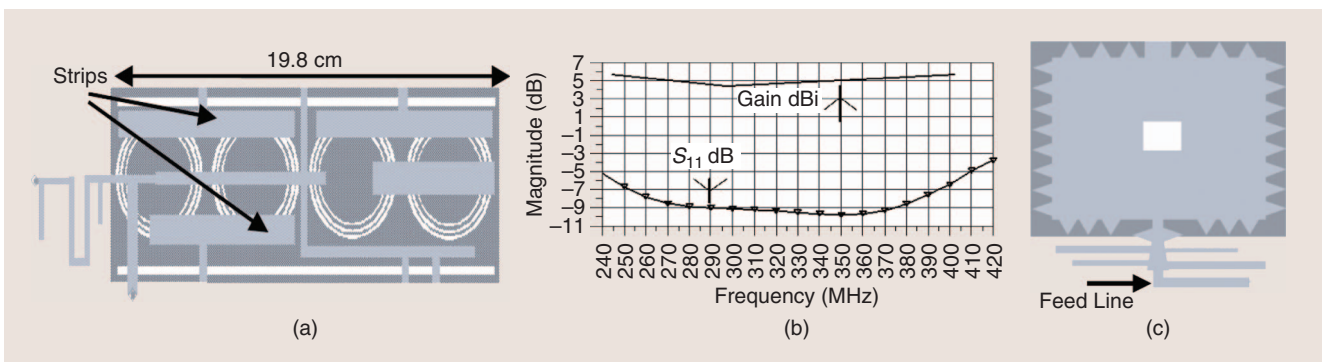


Figure 7. (a) The antenna with metallic strips, (b) the S_{11} and antenna gain, and (c) the fractal patch. Figure 8 presents photos of the antenna in wearable forms.

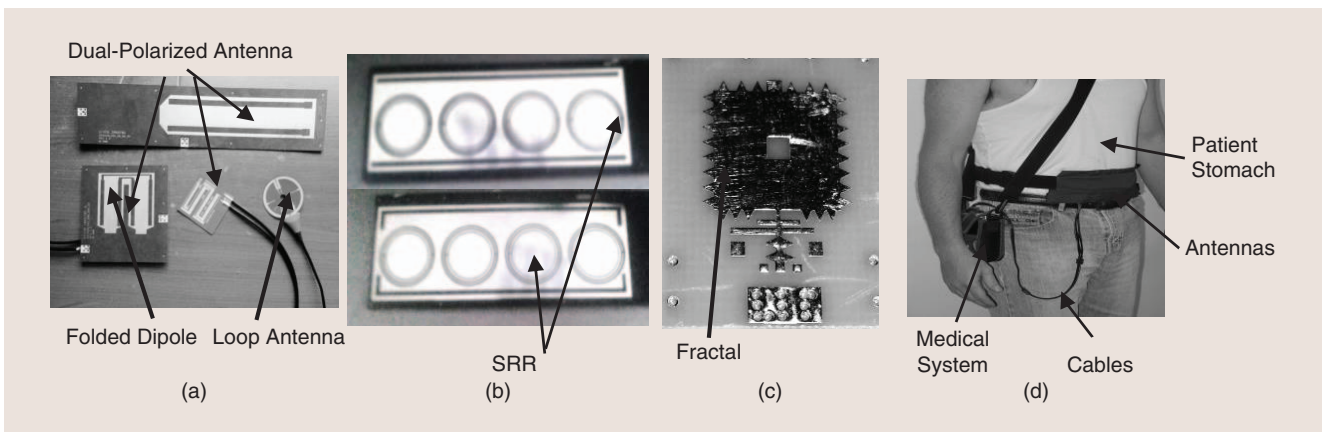


Figure 8. (a) Wearable antennas for medical applications, (b) metamaterial-based antennas, (c) a fractal wearable antenna resonator at 8 GHz, and (d) wearable antennas mounted on patient.

transceiver system-on-chip (SoC) for ultrawide-band (UWB) multiple-input/multiple-output (MIMO) radar uses, with medical, in-wall, and over-the-air applications in mind (such as in its Walabot products); see Figure 9. The 8-mm × 8-mm SoC supports 24 Tx/Rx

channels, operating up to 20 GHz. The application-specific IC supports stepped-continuous-wave (CW) and linear frequency-modulated radar modes. The UWB regime allows submillimeter-wave Tx power, yet distributed amplifiers are used for large bandwidth,

and mixer-based receivers are used for dynamic range. Particular attention was given to the isolation between transceiver elements.

An isolation of 30 dB between adjacent transceivers and greater than 90 dB (!) between opposite sides of the

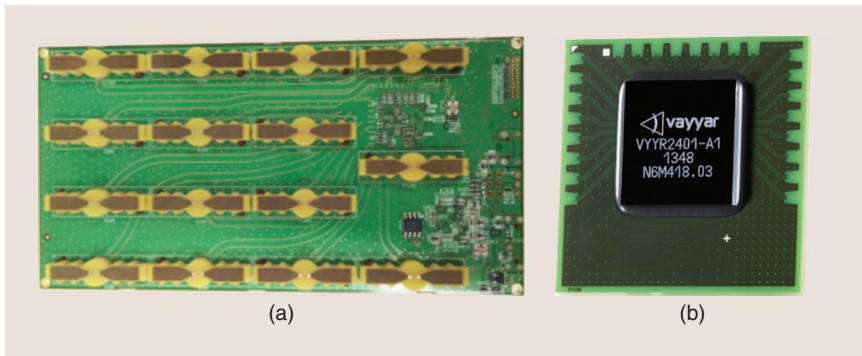


Figure 9. (a) The cell phone-sized Walabot UWB MIMO radar and (b) the Octopus VYYR2401 RFIC in a flip-chip package.

chip was achieved using differential signals, taking advantage of reverse isolation of amplifiers and a meticulous electromagnetic design of the flip-chip package.

The VYYR2401 SoC was designed with modularity in mind and to support larger systems, for example, Vayyar's medical MIMO imaging system, which has approximately 100 antennas. The SoC supports synchronization and reference signal distribution among multiple RFICs to allow synchronous and phase-coherent MIMO signal acquisition with multiple chips.

The microwave capabilities are complemented by the digital portion of the chip, the analog-to-digital converters, the on-chip memory to buffer the acquired responses, and interfaces to stream the acquired data to the host processor. The acquisition is complemented by a suite of calibration and image-formation algorithms.

Vayyar is currently developing millimeter-wave MIMO radar imaging,

with increased per-chip port count, in its next-generation RFIC SoC.

RFIC: Error Vector Magnitude Prediction in the Design Flow

In this section, we present a new method for quantifying the error vector magnitude (EVM) during the RFIC design flow, which is becoming increasingly important, particularly in Tx systems with high-order modulation [8]. This technology has been developed at Rio Systems in Israel.

Traditional RFIC design flow uses CW stimulus to evaluate the signal integrity and nonlinear terms such as third-order intermodulation products and nonlinear compression points of the subsystem. The use of modulating signals in RFIC design flow is not widespread due to 1) the long simulation times whenever a transistor level design with strong nonlinear characteristics is subject to high-order modulations and 2) the need for different design environments.

The realized core IC offers phase and amplitude controls to meet specific beam-forming characteristics that, in most cases, are not optimized to minimum EVM over a wide range of input power levels and multiple circuit conditions. The subsystem and EVM results are shown in Figure 10. EVM below 1.8% in orthogonal frequency-division multiplexing with 64 quadrature amplitude modulation is normally required, which means careful system optimization. Translating stringent EVM requirements into an actual RFIC design flow is of paramount importance to deliver a system with high power efficiency and excellent EVM performance.

An integrated EVM analysis in the RFIC design flow [where the nonlinear amplitude-to-amplitude (AM-AM) modulation and amplitude-to-phase (AM-PM) modulation characteristics at different bias conditions as well as the small-signal and noise parameters are inserted automatically into the model description file and the core IC] was developed. The importance of the integrated EVM analysis in the RFIC design flow, particularly for systems with EVM specifications below -30 dB, has been presented. Without integrating EVM in the RFIC design flow, the complete RF subsystem might become suboptimum in terms of EVM under different input power and bias conditions.

Conclusions

Research in microwave engineering in Israel is taking place in both industry and academy and is an integral part of the country's high-tech activity. This short article reviewed some highlights

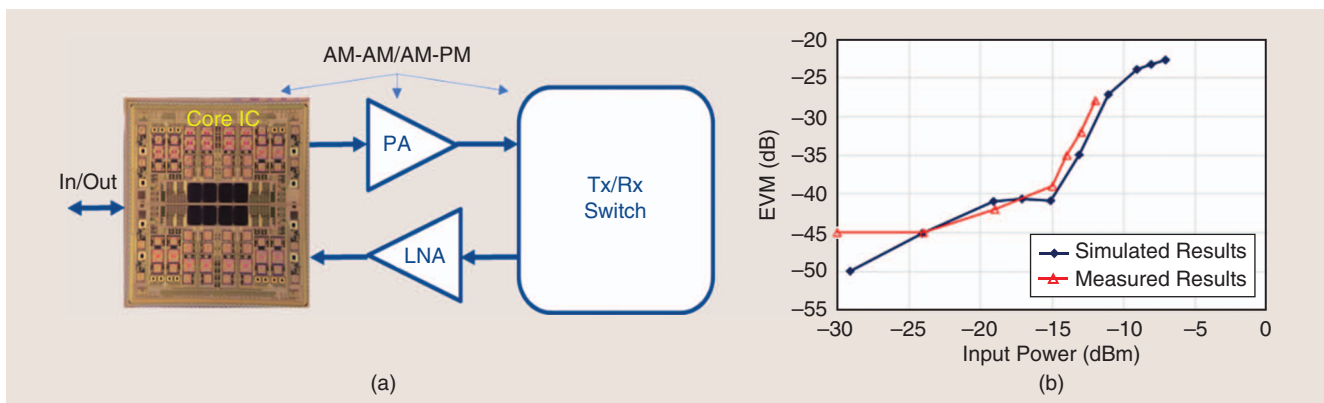


Figure 10. (a) A simplified block diagram of the core IC and (b) the EVM results.

